Engineering of experiment

Chertkova N.V.[1], Spivak A.V.[1], Zakharchenko E.S.[1,2], Litvin Y.A.[1], Kuzyura A.V.[1], Safonov O.G.[1], Efimchenko V.S.[2], Meletov K.P.[1,2] A refinement of the externally heated diamond anvil cell technique for laboratory applications, UDC 53.086; 608.2; 543.424.2

[1]D.S. Korzhinskii Institute of Experimental Mineralogy of Russian Academy of Sciences (IEM RAS), Chernogolovka, [2] Institute of Solid State Physics of Russian Academy of Sciences (ISSP RAS), Chernogolovka (nadezda@iem.ac.ru)

Abstract: In this work, we describe a diamond anvil cell technique with external heating system, which can be used in combination with the common laboratory equipment for *in situ* spectroscopic analysis of the samples at high pressures and elevated temperatures. We further demonstrate its performance in the study of ammonia borane decomposition in the presence of silicate and show optical images and Raman spectra, which were taken during experiments.

Key words: externally heated DAC, in situ experiment, high pressure, Raman spectroscopy

Spectroscopic methods of sample investigation in the diamond anvil cell (DAC), which allow analysis of solid, liquid and gaseous phases *in situ*, are widely applied in the fields of Earth's Sciences, Material Sciences, Chemistry and Physics (Smith & Fang, 2009; Ferraro, 2012). In comparison to laser heating, external heating of the DAC provides an opportunity to avoid large temperature gradients (Dubrovinskaia & Dubrovinsky, 2005) and to reduce the impact of kinetic factors on phase equilibria under investigation (Sinmyo & Hirose, 2010). Using the technological base of the Institute of Experimental Mineralogy of Russian Academy of Sciences, we established and refined an external heating system for the "piston-cylinder" type DAC, designed for optical observations and measurement of Raman spectra at high-pressure conditions.

The DAC had a wide opening of 60° for optical access to the sample during experiments. The cell was placed inside the copper frame, purged with the 98%Ar+2%H_2 gas mixture and cooled with water. Experimental assembly was placed under the optical microscope, connected to the digital camera and Raman spectrometer. The photographs and Raman spectra were taken during heating while the sample was subjected to high pressures.

Performance of the described technique was checked in the test experiments, using fused quartz (SiO_2) and ammonia borane (NH_3BH_3) as the starting materials. The ruby ball, which served as a pressure sensor (Jayaraman, 1986; Ragan et al., 1992), was loaded into the sample chamber together with these materials (Fig. 1a).

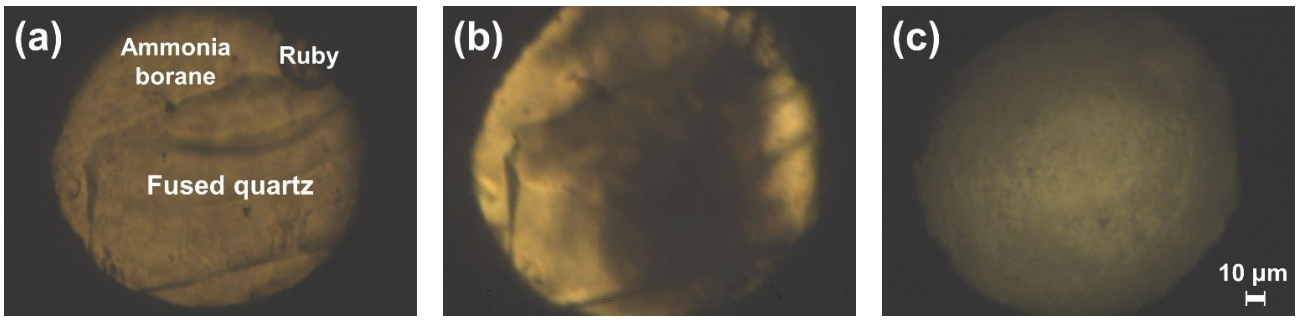

Fig. 1. Optical microphotographs taken during experiment in the externally heated diamond anvil cell at 25 °C and 2.9 GPa (a); 215 °C and 4.5 GPa (b); 252 °C and 4.6 GPa (c).

The phase transitions and steps of decomposition of ammonia borane were monitored visually and checked by Raman spectroscopy. Above 140 °C and 3.7 GPa, the change in Raman spectra of ammonia borane (Fig. 2) coincided with the solid-solid phase transition from the phase with orthorhombic $Cmc2_1$ symmetry (Chen et al., 2010) to the phase with *Pnma* symmetry (Nylén et al., 2013). The first step of decomposition was clearly seen in the optical images at 215 °C and 4.5 GPa (Fig. 1b), accompanied by darkening of ammonia borane and appearance of hydrogen droplets. Molecular hydrogen was preserved in the sample chamber up to the highest experimental temperatures and detected in the run products after quenching.

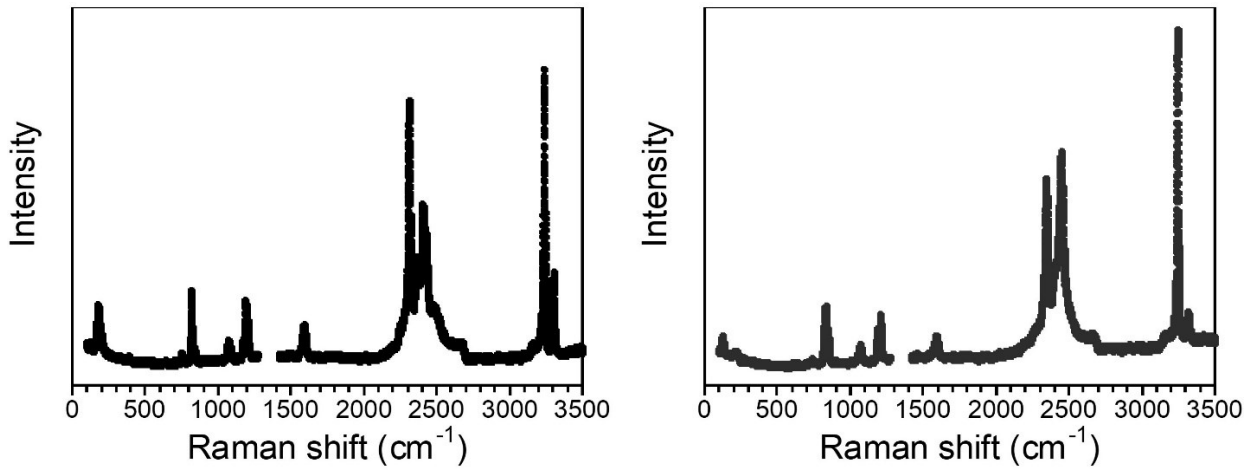

Fig. 2. Raman spectra of ammonia borane (NH_3BH_3) measured *in situ* at 25 °C and 2.9 GPa (left) and at 151 °C and 3.8 GPa (right).

Experiments showed applicability of the developed method for high-pressure studies of various materials, including highly mobile fluids, at elevated temperatures. The compact size of the experimental cell makes it suitable for *in situ* spectroscopic investigations using common laboratory equipment.

This work was carried out within the state task of the D.S. Korzhinskii Institute of Experimental Mineralogy of Russian Academy of Sciences (AAAA-A18-118020590140-7).

This work was carried out with the support of the Russian Science Foundation (project No. 20-77-00079) and partially within the state task of the D.S. Korzhinskii Institute of Experimental Mineralogy of Russian Academy of Sciences (AAAA-A18-118020590140-7).

References

Chen J., Couvy H., Liu H., Drozd V., Daemen L. L., Zhao Y., Kao C.-C. In situ X-ray study of ammonia borane at high pressures// International journal of hydrogen energy. 2010. Vol. 35. № 20. P. 11064-11070.

Dubrovinskaia N., Dubrovinsky L. Internal and external electrical heating in diamond anvil cells. In Advances in High-Pressure Techniques for Geophysical Applications. 2005. P. 487–501. Elsevier.

Ferraro J. R. Vibrational spectroscopy at high external pressures: the diamond anvil cell. Elsevier. 2012.

Jayaraman A. Ultrahigh pressures// Review of Scientific Instruments. 1986. Vol. 57. № 6. P. 1013-1031.

Nylén J., Eriksson L., Benson D., Häussermann U. Characterization of a high pressure, high temperature modification of ammonia borane (BH3NH3)// Journal of Chemical Physics. 2013. Vol. 139. № 5. P. 054507.

Ragan D. D., Gustavsen R., Schiferl, D. Calibration of the ruby R1 and R2 fluorescence shifts as a function of temperature from 0 to 600 K// Journal of Applied Physics. 1992. Vol. 72, № 12, P. 5539-5544.

Sinmyo R., Hirose K. The Soret diffusion in laser-heated diamond-anvil cell// Physics of the Earth and Planetary Interiors. 2010. Vol. 180. P. 172-178.

Smith R. L., Fang Z. Techniques, applications and future prospects of diamond anvil cells for studying supercritical water systems// The Journal of Supercritical Fluids. 2009. Vol. 47. № 3. P. 431-446.

Lakshtanov L.Z., Karaseva O.N. Study of the mechanisms of chalk recrystallization.

UDC 550.4.02

IEM RAS, Chernogolovka, (olga@iem.ac.ru)

Abstract. For each chalk sample, the induction period of the homogeneous nucleation of a supersaturated $CaHCO_3$ solution, obtained by dissolving the samples at pCO_2 = 1 atm, was measured in the process of balancing to atmospheric CO_2 pressure. Crystallization ability of chalks was correlated with the content of polysaccharides and cyclic hydrocarbons. Using the vapor adsorption method, the effect of biopolymers (Alg and pAsp) adsorbed on calcite on free surface energy was studied. Adsorbed biopolymers reduce the effective free energy of the surface, and therefore, for high supersaturation, reduce the nucleation rate.

Keywords: chalk, calcite, nucleation, induction period, surface free energy

The study of the effect of organic matter on the surface of natural chalk on their recrystallization was continued. We used calcite powder ($CaCO_3$, Sigma) and Maastrichtian chalk samples taken from water and gas-saturated deposits of the North Sea, as well as from the Aalborg open pit, Denmark.

For each sample, the induction period of homogeneous nucleation of a supersaturated $CaHCO_3$ solution obtained by dissolving chalk samples at pCO_2 = 1 atm was measured in the process of re-equilibration to atmospheric pressure of carbon dioxide. Correlation of the crystallization ability of chalk with the content of polysaccharides and cyclic hydrocarbons has been carried out. Fig. 1

shows the values of the induction period of homogeneous nucleation as a result of CO_2 degassing from solutions saturated with calcite, as well as various chalk samples at a partial pressure of CO_2 = 1 atm, and then placed under atmospheric conditions ($pCO_2 = 10^{-3.5}$). (Gauthier et al., 2012; Hamdi et al., 2016).

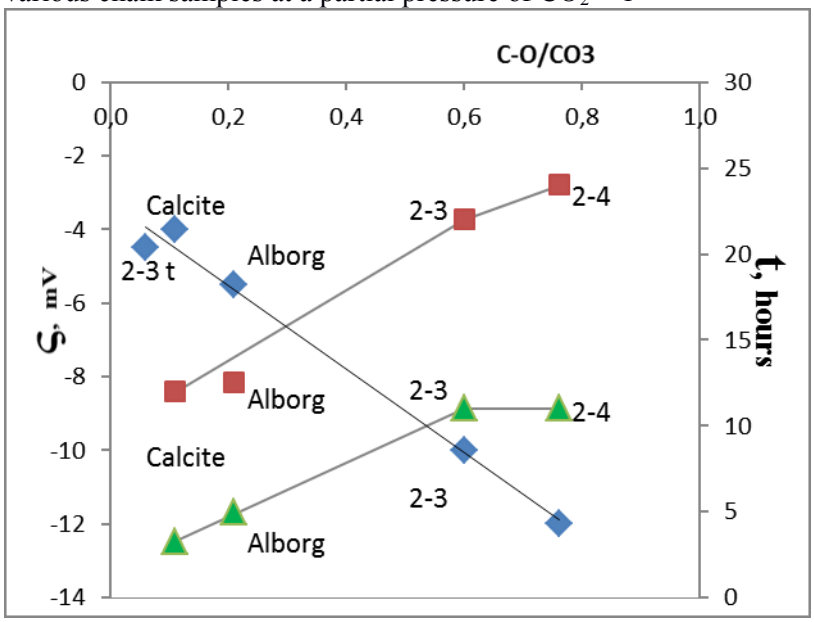

Fig. 1. ζ-potential (rhombs) of calcite and chalk samples at pH 9.6 as a function of the relative surface concentration of C-O bonds. Chalk 2-3t had been treated with H_2O_2 (Belova et.al 2012) and induction time for homogeneous nucleation during CO_2 degassing from solution saturated with respect to calcite as well various chalk, monitored by pH drop (squares) and by turbidity (triangles).

During CO_2 degassing, the supersaturation of the solution with respect to calcite, S, is not constant, but increases (for calcite, S = 1 to 5.9 at t = 0 to t_{ind}, for Chalk 2-3, S = 1 to 8.1 at t = 0 to t_{ind}), so the measured values of the induction period cannot be used in the nucleation theory equations to calculate, for example, the free surface energy of the resulting phase. However, these induction period values can be used to compare different samples of chalk and calcite. The induction period identified by the pH jump is significantly higher than that one measured from turbidity, which is explained by much slower degassing. There is almost 2 times less contact area of the solution with the air because of the pH-microelectrode introduced into cuvette. However, the curves for the induction period data (Fig. 1), obtained by different methods, have the same shape.

Figure 1 shows that the induction period for homogeneous nucleation for all samples, as well as the values of ζ - potential, correlate well with the relative surface concentration of C-O bonds, i.e. with the concentration of polysaccharides on the surface of the samples. For chalk samples from the North Sea Basin (Samples 2-3 and 2-4), the induction period is much longer than for pure calcite or for the Aalborg chalk, which is explained by a significantly higher surface concentration of organic matter, in particular, polysaccharides, on the surface of these samples.

Using the vapor adsorption method, the effect of biopolymers adsorbed on calcite on the free surface energy was studied. Samples of polymer adsorbed calcite were prepared for precipitation experiments as well as for vapor adsorption measurements. Calcite powder, weighing 2 g was placed in 50 ml of a solution saturated with calcite at pH 8.5 and a certain amount of biopolymer solution. After 2 or 24 hours, the suspension was filtered, washed with a calcite-saturated solution and freeze dried.

The results for determination of total surface energy, γ_s, and free energy of the calcite - water interface, γ_{sw}, are listed in Table 1. The relative error in the estimation of the amount of adsorbed vapor and therefore work of wetting is 2%. For a pure calcite sample, the determined total surface energy of γ_s is in good agreement with our previous results (Lakshtanov et al. 2015). The free interface energy, γ_{sw}, was obtained from the equation:

$$\gamma^{SW} = \gamma^{S} + \gamma^{L} - W_A,$$ where W_A is work of adhesion.

We estimated the free surface energy of calcite - water to be 129.3 mJ/m^2, which is close to 120 mJ/m^2 reported by Söhnel and Mullin (1982). It should be noted that the results for the total surface energy and the distribution of its polar and dispersion components depend on the choice of the reference vapor. We used ethanol in our measurements.

When the biopolymer was adsorbed on calcite, we observed a decrease in the total surface energy and a change in the distribution of the dispersion and polar components. The polar component decreased, while the dispersion component increased. The effect was more pronounced if the biopolymer was adsorbed for a longer period of time, as well as at a higher concentration of the biopolymer. The decrease in the energy of the free interface is shown in Fig. 2.

Table 1 . Surface energies for calcite with adsorbed Alg and pAsp.

Sample	Conc., g/L	Time of adsorption, days	Surface energy, y^s, mJ/m^2			Interface energy y^{sw}, mJ/m^2
			Dispersive	Polar	Total	
Pure calcite	-	-	2.9	328.3	331.2	129.3
Calcite + Alg	0.013	2	81.5	211.9	293.4	74.0
	0.1	2	12.3	331.6	343.9	123.9
	0.17	2	76.9	204.3	281.3	68.0
	0.013	24	53.0	261.8	314.8	88.5
	0.1	24	91.0	199.2	290.2	72.3
	0.1	24	90.0	246.3	336.3	96.3
	0.17	24	39.3	262.4	301.8	84.6
	0.17	24	18.3	327.1	345.4	119.9
Calcite + pAsp	0.0043	2	33.0	260.3	293.3	82.0
	0.0087	2	49.7	176.7	226.4	43.5
	0.025	2	36.0	218.3	254.2	60.1
	0.0435	2	31.1	236.0	267.1	68.4
	0.0435	2	36.8	285.8	322.7	97.3
	0.0043	24	18.9	234.8	253.7	67.1
	0.0087	24	25.6	159.9	185.6	30.5
	0.025	24	56.0	164.5	220.4	40.2
	0.0435	24	93.9	102.4	196.3	34.1
	0.87	24	1.8	947.5	949.4	569.8

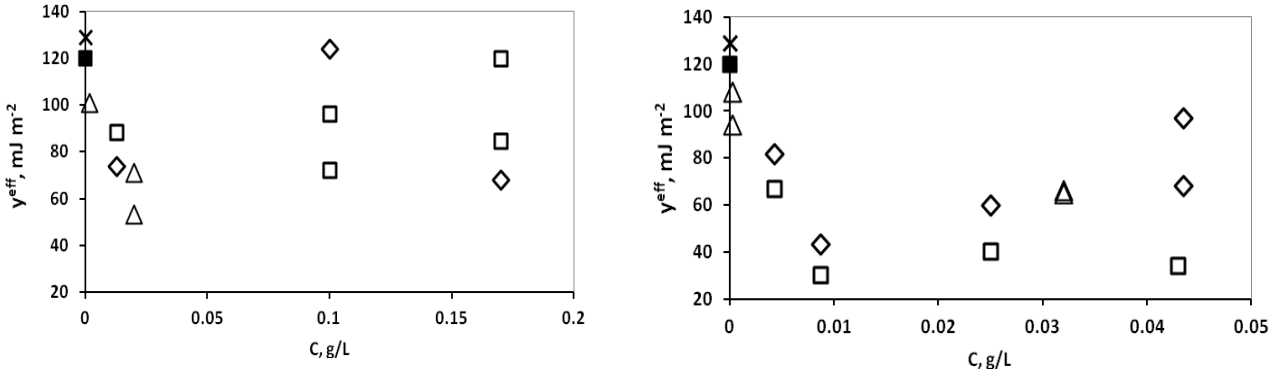

Fig. 2. The effective interface free energy,γ^{eff}, for calcite adsorbed polymers. A) – for Alg and B) – for pAsp (obtained by several method) versus polymer concentration: triangles, from precipitation kinetics; squares, from vapour adsorption measurements (24 h polymer adsorption); rhombi, from vapour adsorption measurements (2 h polymer adsorption); crosses, from vapour adsorption measuremets (pure calcite); filled squares, theoretical value, γ_{cw}, for a pure calcite-water interface (Söhnel and Mullin 1978).

The effect is more significant for pAsp than for Alg, and also with higher adsorption times. For example, the free energy of the calcite - water interface decreases from 129.3 mJ/m2 for pure calcite to 30.5 mJ / m2, when pAsp (8.7 mg / L) is adsorbed within 24 hours. However, with an increase at pAsp concentration (to 870 mg/l), the surface energy is very high due to the significant absorption of water. This phenomenon can be explained by the fact that at high pAsp concentrations, complete surface coverage is achieved, and the calcite - water interface disappears. In this case, we observed only the interaction of water molecules with pAsp, which is known to form hydrogels to retain water (Meng et al., 2015); high water absorption leads to incorrect surface energy values.

The adsorbed biopolymers decrease the effective free energy of the surface, and, therefore, for high supersaturation, they decrease the nucleation rate, that is, increase the induction period, as we observed in the experiments.

References

Belova D.A, Johnsson A, Bovet N, Lakshtanov L.Z, Stipp S.L.S. (2012) The effect on chalk recrystallization after treatment with oxidizing agents. *Chem. Geol.* 291: 217–223.

Gauthier G., Chao Y., Horner O., Alos-Ramos O., Hui F., Lédion J., Perrot H. (2012) Application of the Fast Controlled Precipitation method to assess the scale-forming ability of raw river waters. *Desalination* 299: 89-95.

Hamdi R., Khawari M., Hui F. and Tlili M. (2016) Thermodynamic and kinetic study of CaCO3 precipitation threshold. *Desalination and Water Treatment* 57: 6001-6006.

Lakshtanov L.Z., Belova D.A., Okhrimenko D.V., Stipp S.L.S. (2015) Role of alginate in calcite recrystallization. *Cryst. Growth Des*. 15: 419-427

Meng H, Zhang X, Chen Q, Wei J, Wang Y, Dong A, Yang H, Tan T, Cao H (2015) Preparation of poly(aspartic acid) supera- bsorbent hydrogels by solvent-free processes. J Polym Eng 35: 647–655

Söhnel O., Mullin J.W. (1982). *J. Cryst. Growth* 60: 239–250

Molchanov[1] V.P., Medkov[2] M.A. Ways of industrial development of gold-ilmenite placers of the sikhote-alin with the use of pyro- hydrometallurgical methods

[1]Far East Geological Institute, Far Eastern Branch of the RAS, Vladivostok, Russia, (*vpmol@mail.ru*),
[2] Institute of Chemistry, Far Eastern Branch of the RAS, Vladivostok, Russia.

Abstract. During our research of capabilities of pyro-hydrometallurgical methods of enrichment we used the material of magnetic and nonmagnetic fraction of the gravity concentrate of gold-ilmenite placers of the Ariadnensky ultrabasic massif (Primorye). When extracting TiO_2 from ilmenite magnetic fraction using the traditional vitriolic method we replaced the liquid sulfating agent with solid ammonium sulfate. Water leaching at a temperature of 360^0 C allowed us to transfer all of the titanium and most of iron as very soluble in water double salts. When extracting gold from non magnetic fraction we used thiocarbamide-thiosulphate leaching solutions (metal extraction grade equaled 89-90%) instead of cyanides. The conducted research allowed us to develop technology basics for gold-ilmenite placers' processing by methods of gravity, electromagnetic separation, pyro- hydrometallurgy thus observing the principles of rational environmental management and safety.

Keywords: *titanium, gold, gravity, electromagnetic separation, pyro-hydrometallurgy, gold-ilmenite placers, Primorye.*

Primorye has long been known for its gold deposits (Lelikov et al., 2013). Noble metals (BM) have been mined here since the time of the Bohai kingdom (VIII-X vv). To date, most of the placer deposits of BM have their resource potential almost completely exhausted. Under these conditions, the strengthening of the region's raw material base is associated with complex manifestations of exogenous mineralization. These include titanium-bearing placers of the Sikhote-Alin orogenic belt, in which BM minerals are associated components. Most of them are spatially and genetically associated with synorogenic intrusions of basite-ultrabasites. The main directions of their development are in-depth mineralogical and geochemical assessment, integrated use and deep processing of raw materials. An example of this approach is the ilmenite placers of the Ariadne massif of ultrabasites, in which BM minerals were first discovered by the authors (Molchanov et al., 2017).

Ariadne massif of basic ultrabasites, located in the middle reaches of the river. Robin (the catchment area of the Ussuri River, a tributary of the Amur River), belongs to the group of differentiated intrusions of the Ariadne metallogenic belt confined to the Samarkinsky terrain of the Jurassic accretionary prism. Upper Jurassic turbidites and olistostromes of accretionary prism with inclusions of Late Paleozoic and Lower Mesozoic oceanic flints, schists, limestones and basalts that are broken through by the Aruadite-Early Basin and Aruadite basenites are involved in the geological structure of the Ariadne ore-placer junction, which coincides with the contours of the homonymous massif. Its southern part is composed of peridotites and olivine pyroxenites, to the north ilmenite and hornblende gabbro prevail, turning into diorites, monzodiorites and syenites. The above stratified and magmatic formations, in turn, are penetrated by late granitoids, dikes of the main and acidic composition of the Late Cretaceous (Geodynamics ..., 2006).

The Ariadna massif of ultrabasite basites located in the middle course of the Malinovka River (the catchment area of the Ussuri River, a tributary of the Amur River) belongs to the group of differentiated intrusions of the Ariadna metallogenic belt confined to the Samarka terrane of the Jurassic accretionary prism. Upper Jurassic turbidites and olistostromes of accretionary prism with inclusions of late paleozoic and lower mesozoic oceanic flints, schists, limestones and basalts that are broken through by the Aruadite-Early Basin and Aruadite basenites are involved in the geological structure of the Ariadne ore-placer junction, which coincides with the contours of the homonymous massif. Its southern part is composed of peridotites and olivine pyroxenites, to the north ilmenite and hornblende gabbro prevail, turning into diorites, monzodiorites and syenites. The above stratified and magmatic formations, in turn, are penetrated by late granitoids, dikes of the main and acidic composition of the Late Cretaceous (Geodynamics ..., 2006).

The Ariadne massif produces a number of large titanium-bearing placers. Thus, the length of placers of the Todokhov river and its right stream of the Potapov river is 4,8 km and 1,2 km, respectively, with a width of up to 520 m and 280 m, an average productive reservoir capacity of 7,4 m and an ilmenite content of up to 375,5 kg/m3. The balance reserves of TiO_2 of category C_1+ C_2 as of 01.01.2019 are 702 thousand tons, and the forecast resources reach 500 thousand tons.

Preliminary mineralogical studies of the initial Sands have shown that titanium in placers is represented exclusively by ilmenite, which is the main mineral for industrial extraction. The material composition of the initial productive Sands is characterized by a predominance of TiO_2 (19,55

mas.%), SiO_2 (19,72 mas.%), Fe_2O_3 (to 19,9 mas.%), MgO (4,48 mas.%). Rare, rare earth and noble metals are recorded among the permanent impurities. The rare element composition is characterized by the presence of Ta (up to 100 g/t) and Nb (up to 11 g/t). Concentrations of rare earth elements are slightly higher than the Clark level. The content of Au and Pt rarely exceeds 0,1 g/t, while Pd is present in quantities up to 1,1 g / t. It is impossible not to pay attention to the high level of concentration of V (up to 730 g/t), Co (340 g/t), Zn (230 g/t).

After that, the concentrate samples were enriched at the gravity plant. The resulting concentrates were separated into magnetic and non-magnetic fractions by electromagnetic separation. The material composition of gravity concentrates is characterized by a high yield of the magnetic fraction (93-95 mas.%) and low-non-magnetic one (5-7 mas.%). The basis of the magnetic fraction is ilmenite (up to 95%). Occasionally, titanomagnetite grains are fixed. The chemical composition of the magnetic fraction is characterized by high TiO_2 concentrations (39,79 mas.%), Fe_2O_3 (34,47 mas.%), MgO (1,8 mas.%), MnO (0,42 mas.%). It should be noted that increased concentrations of SiO_2, Al_2O_3, and CaO are probably associated with the presence of ilmenite splices with amphiboles, pyroxene, and plagioclase in the fraction. A distinctive feature of the magnetic fraction material is the high level of presence of the following elements (g/t): V – 800, Nb - 210, Nd-100, Co - 290, Cu - 490 и Zr - 280.

The non-magnetic fraction is essentially a mixture (mas.%) anorthite (36,9), quartz (24,3), hornblende (17,6), sphene (15,4) and zircon (3,8). In addition, small amounts of monazite, rutile, and apatite are present. Of the ore minerals, sulfides (single grains of pyrite, arsenopyrite, antimonite, and galenite) and native metals (gold, platinum, zinc, and Nickel) predominate. Non-magnetic concentrate is characterized by the following chemical composition (mas.%): SiO_2-49,6; CaO -13,2; Al_2O_3-11,0; TiO_2-9,4; ZrO_2 – 4,23; P_2O_5-4,15; Fe_2O_3 – 3,23; MgO-1,84; Na_2O-1,67; K_2O-1,18; V_2O_5 – 0,096.Trace elements of the concentrate can be divided into two groups. The first of them includes rare and rare earth elements (g/t): Hf - 830, Ce - 320, Y - 220. The second group includes precious metals-Au, Ag and Pt, whose concentrations vary within the range of 0,5-3,0 g/t.

The objectives of our research were to study the possibilities of industrial development of gold-ilmenite placers using pyro-hydrometallurgy methods. In line with this problem, a large amount of experimental research has been carried out, including studies of the solid-phase interaction of a material of the magnetic fraction of a gravitational concentrate (almost completely composed of ilmenite) with ammonium sulfate. As it is known (Rare and scattered elements..., 1996, Patent of the Russian Federation, 2015), ilmenite is relatively easy to decompose by acids, so the sulfuric acid method is widely used for its opening. This is the oldest industrial method for extracting TiO_2 from ilmenite, which consists in converting ilmenite to soluble sulfates. The process consists of three stages and a large number of operations (drying the concentrate to a moisture content of 0,5%, oleum sulfation at 80-210^{0}C with rapid release of gases and splashing of the reaction mixture, aging of the porous product, leaching and reduction of iron in solutions with cast iron chips, and many others). Derived from the acid treatment solution is purified from iron by crystallization of ferrous iron when it is cooled and then directed to the hydrolysis. When calcining the hydrolysis sediment, TiO_2 is obtained.

The use of sulfuric acid technology is associated with a large consumption of concentrated sulfuric acid (4000-4500 kg/t of the target product) and, in addition, leads to significant pollution of the environment, since hundreds of thousands of tons of sulphate-containing waste in the form of $CaSO_4$ and acidic wash waters are dumped annually. Therefore, it is of interest to study the possibility of replacing a liquid sulfatizing reagent with a solid one, in particular, ammonium sulfate $(NH_4)_2SO_4$ during sulfuric acid dissection of ilmenite. During the experiment, it was established:

1. The interaction of the concentrate with $(NH_4)_2SO_4$ starts when the temperature of thermal decomposition of $(NH_4)_2SO_4$ is (300^{0}C) and in the temperature interval 300-360^{0}C there takes place a mixture of double salts of ammonium sulphate and iron compounds $(NH_4)_2Fe_2(SO_4)_3$ and $NH_4Fe(SO_4)_2$ and ammonium sulphate and titanyl composition $(NH_4)_2TiO(SO_4)_2$.

2. An increase in the interaction temperature of ilmenite concentrate with $(NH_4)_2SO_4$ above 360^{0}C leads to the thermal decomposition of double ammonium and titanyla sulfates, as well as ammonium and iron to sulfates and then oxides..

3. Water leaching of the product of interaction of ilmenite concentrate with $(NH_4)_2SO_4$ at a temperature of 360^{0}C allows to transfer almost all titanium and the bulk of iron into solution in the form of double salts that are well soluble in water.

After passing the stage of electromagnetic separation, the non-magnetic components of the gravity concentrate, including the bulk of the BM, served as the raw material for hydrometallurgical research. We have previously established (Molchanov et al., 2004) that gold from this type of raw material is effectively extracted when leaching with thiocarbamide-thiocyanate solutions. Since the relatively high price of thiocarbamide and its losses at the stages of filtration and extraction of gold prevent the widespread industrial use of

thiocarbamide dissolution of BM, the process of extracting gold from thiocarbamide solutions using liquid extraction is proposed as a possible way to reduce the loss of thiocarbamide during the processing of gold-containing concentrates. In addition, the use of liquid extraction at the stage of extracting gold and silver from leaching solutions allows selective extraction of precious metals with additional separation from impurities. The only problem that occurs in this case is the output of Fe, As and Cu accumulating in the turnover. However, this problem is solvable, since the technology provides for complete neutralization of circulating solutions with lime after five to seven leaching cycles to reduce the overall salt background.

Tributyl phosphate, diphenylthiourea and their mixture were used as extractants. It was found that the thiocarbamide complexes of gold formed during leaching are practically not extracted by individual extractants and are poorly extracted by a mixture of diphenylthiourea with tributyl phosphate. However, gold is extracted with tributyl phosphate, as well as a mixture of diphenylthiourea with tributyl phosphate with high distribution coefficients when introduced into thiocarbamide solutions of thiocinate ions. It was found that the isolation of sodium thiocinate in thiocarbamide solutions does not impair the recovery of gold at the leaching stage and, most importantly, the extraction is not accompanied by a transition to the organic phase of thiocarbamide, since gold is extracted in the form of thiocinate complexes. Thus, the use of liquid extraction at the stage of gold extraction from leaching solutions allows to avoid losses of thiocarbamide.

Tributyl phosphate, diphenylthiourea and their mixture were used as extractants. It was found that the thiocarbamide complexes of gold formed during leaching are practically not extracted by individual extractants and are poorly extracted by a mixture of diphenylthiourea with tributyl phosphate. At the same time, gold is extracted by tributyl phosphate, as well as by a mixture of diphenylthiourea with tributyl phosphate with high distribution coefficients when thiocarbonate ions are introduced into thiocarbamide solutions. It was found that the isolation of sodium thiocinate in thiocarbamide solutions does not impair the recovery of gold at the leaching stage and, most importantly, the extraction is not accompanied by a transition to the organic phase of thiocarbamide, since gold is extracted in the form of thiocinate complexes. Thus, the use of liquid extraction at the stage of gold extraction from leaching solutions allows to avoid losses of thiocarbamide.

It should be noted that if there are associated components in the leaching solutions, the latter almost completely pass into the organic phase. In this regard, we have attempted to separate all metals from the organic phase, bypassing the washing stage. The studies have shown that the most effective metals from the organic phase are precipitated by sodium borohydride. Thus, when the extract is treated with a solution containing 0,5 mol/l $NaBH_4$, a black precipitate appears at the phase interface. In this case, the extractant is not destroyed and does not lose the ability to extract the BM. The filtered interfacial sediment was subjected to oxidative melting after washing with concentrated nitric acid. The end-to-end extraction of gold from raw materials according to this scheme is 89-90%.

In conclusion, we note that the proposed technical solutions are only the first step in the development of gold-ilmenite placers in the South of the Russian Far East. It is obvious that further research needs to be carried out in the direction of complex processing of gold-titanium-bearing sands, which will reduce the cost of obtaining individual products and ensure higher production efficiency.

The work was supported by RFBR grant № 20-05-00525.

References

Geodynamics, magmatism and metallogeny of the East of Russia / edited by A I. Khanchuk. Kn.1. Vladivostok: Dalnauka, 2006. 572 p.

Lelikov E P. Askold Island: geological structure and gold-bearing // Vestnik DVO RAN. 2013. №. 6. P. 198-204.

Molchanov V P, Androsov D V. Minerals of noble metals of the Ariadne massif of hyperbasites (Primorye) // Geology and mineral resources of the North-East of Russia. Yakutsk: NEFU. 2017. P.142-146.

Molchanov V P, Medkov M A, Khomich V G, Belobeletskaya M V. Studies of technogenic placers of Primorye as a source of additional extraction of precious metals // Geochemistry.2004. №. 6. P. 684-688.

Rare and scattered elements. Chemistry and technology / edited by S S. Korovin. Kn. II. Moscow: MISIS, 1996. 461 p.

Gerasimova L G, Kasikov A G, Bagrova E G. RF Patent № 2571904. Method for processing titanium-containing material. Publ. 27.12.2015.